Multi-stimuli Responsive Reversible Crosslinking-decrosslinking of Concentrated Polymer Brushes

*Xuan Ming Sim,[‡] Chen-Gang Wang,[‡] Xu Liu and Atsushi Goto**

Division of Chemistry and Biological Chemistry, School of Physical and Mathematical Sciences, Nanyang Technological University, 21 Nanyang Link, 637371 Singapore

Abstract. Poly(furfuryl methacrylate) (PFMA) brushes were crosslinked using bismaleimide crosslinkers *via* the Diels-Alder (DA) reaction at 70 °C, generating crosslinked PFMA brushes (PFMA brush gels). The crosslinked PFMA brushes were decrosslinked at 110 °C *via* the retro-Diels-Alder (rDA) reaction, offering the temperature-responsive reversible PFMA brush gels. The wettability of the brush was tunable by the crosslinking and decrosslinking. The use of a disulfide containing bismaleimide as a crosslinker gave the S-S bond at the crosslinking point. The S-S bond was cleaved upon thermal or photo stimulus and regenerated through oxidative stimulus, offering another reversible decrosslinking/crosslinking pathway of the PFMA brush gel. The use of photo stimulus together with photomasks further offered patterned brushes with the crosslinked and decrosslinked domains. The combination of the DA/rDA reactions and the reversible S-S bond cleavage provided multi-stimuli-responsive brush gels for switching the surface properties in unique manners. The reversible crosslinking, multi-responsiveness, access

to patterned structures, and metal-free synthetic procedure are attractive features in the present approach for creating smart functional surfaces.

KEYWORDS: polymer brush, polymerization, stimuli-responsive crosslinking and decrosslinking, surface patterning, functional surface

INTRODUCTION

Stimulus-responsive smart surfaces, which change the surface properties triggered by external thermal, acidic/basic, chemical, electrical or optical stimulus, are finding extensive applications on biomolecular adsorption/desorption, molecular sensing, self-cleaning, and so forth.[1−4] The fabrication of polymer brushes on surfaces is an effective approach for surface modification.[5−9] Stimulus-responsive polymer brushes offer smart surfaces bearing switchable functions and morphologies upon stimulus.[10,11]

Surface-initiated living (or reversible-deactivation) radical polymerization, in which the polymer chains grow from the initiators bound on a solid surface, is a useful method to fabricate well-defined polymer brushes.[6,12−14] Our research group developed an organocatalyzed living radical polymerization, termed reversible complexation mediated polymerization (RCMP), using an alkyl iodide (R−I) as an initiator and an organic molecule as a catalyst.[15−22] Mechanistically, polymer-iodide dormant species (polymer−I) is supposed to coordinate a catalyst (A^+I^-) *via* a halogen bonding to form a complex (polymer−I···catalyst), which reversibly generates a propagating radical (polymer$^\bullet$) (Scheme 1a). RCMP is amenable to a wide range of monomers and can afford concentrated polymer brushes with high graft density (σ) and surface occupancy

($\sigma^* \geq 10\%$).[23,24] The high surface occupancy propels the polymer chains towards extension, leading to unique properties such as high elasticity, ultra-low friction, and super-antifouling against proteins and microorganisms.[25] Such properties of concentrated polymer brushes are different from those of semi-diluted or diluted brushes prepared by conventional radical polymerization or grafting-to methods.

Scheme 1. (a) Reversible Activation in Reversible Complexation-Mediated Polymerization (RCMP); (b) Reversible Diels-Alder Reaction between Furan and Maleimide Moieties.

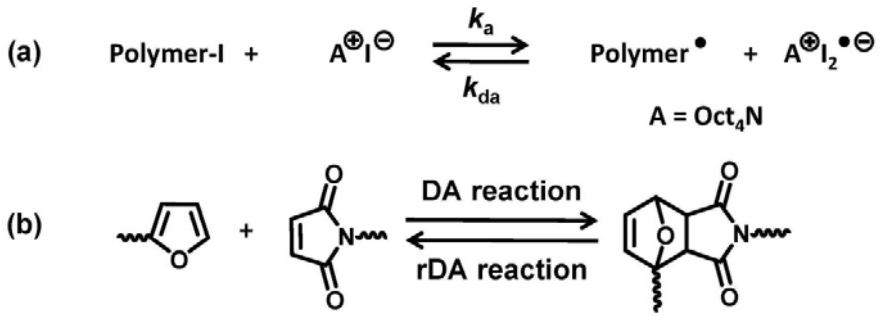

Crosslinked polymer brushes, also known as polymer brush gels, exhibit the properties of both polymer brushes and gels and find unique biomedical applications on interface lubrication, tissue engineering, and anti-fouling coating.[26−31] In comparison to uncrosslinked polymer brushes, polymer brush gels display superior mechanical strength, solvent resistance, anti-corrosion, and durability, exhibiting applications on surface lubrication and interfacial catalysis.[32−37] Reversibly crosslinked polymer brushes, which are crosslinked and decrosslinked *via* external stimuli, can offer a useful approach for controlling the mechanical, biological, and physicochemical surface properties and may find potential applications on electrolyte materials and biomedical interface engineering.[38−40] Whereas reversibly crosslinked polymer brushes are interesting materials, only scarce examples have been reported.

The Diels–Alder (DA) reaction is an effective "click" reaction used in organic synthesis and polymer chemisty.[41−45] In the DA reaction, a [4+2] cycloaddition reaction occurs between an electron-rich conjugated diene (*e.g.*, furan and its derivatives) and an electron-poor alkene (*e.g.*, maleimide and its derivatives) to form a six-membered ring structure (Scheme 1b). An attractive feature of the DA reaction is its thermal reversibility. Upon heating, the six-membered ring structure undergoes a retro-Diels-Alder (rDA) reaction to yield the original diene and alkene. The DA and rDA reactions have widely been used for the preparation and functionalization of polymer materials.[42−44,46] Several examples have also been reported to utilize the DA reaction in polymer brush applications.[47−52]

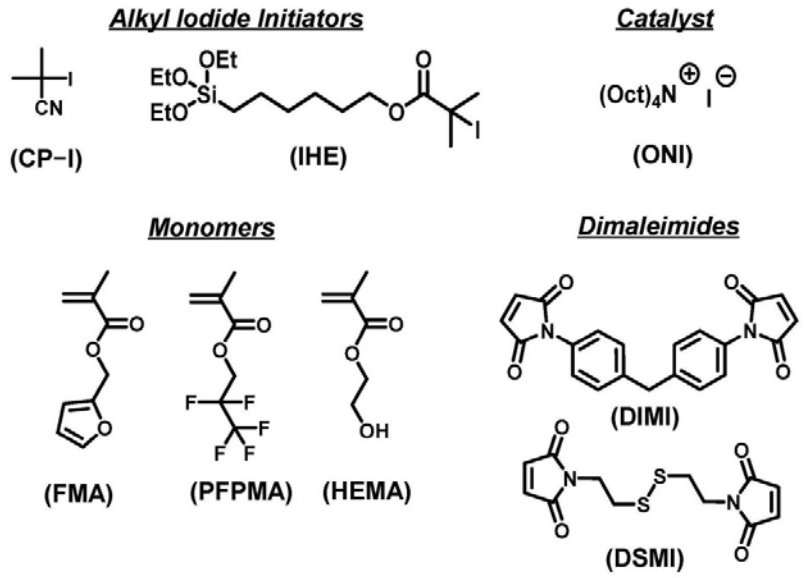

Figure 1. Structures of alkyl iodides, a catalyst, monomers, and dimaleimides used in this work.

Scheme 2. Schematic Illustration of Synthesis of PFMA Brush and Reversible Crosslinking and Decrosslinking of PFMA Brush via DA and rDA reactions.

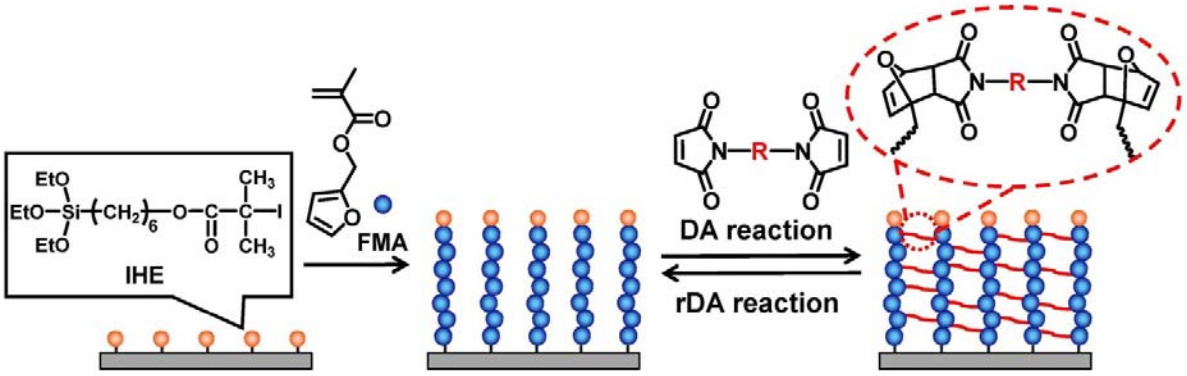

The unique reversibility of the DA and rDA reactions inspired us to create stimuli-responsive surfaces *via* crosslinking and decrosslinking of polymer brushes. In the present work, we used a furan-containing monomer, *i.e.*, furfuryl methacrylate (FMA, Figure 1) and prepared concentrated poly(furfuryl methacrylate) (PFMA) brushes by means of surface-initiated RCMP. The PFMA brushes exhibited two different hydrophobicities (contact angles) switched *via* the crosslinking (DA) (70 °C) and decrosslinking (rDA) (110 °C) reactions with a bismaleimide crosslinker, i.e., 4,4'-bismaleimidodiphenylmethane (DIMI, Figure 1) (Scheme 2). The modulation of the hydrophobicity was repeatable over many cycles.

Furthermore, in the present work, we used bis(2-maleimidoethyl) disulfide (DSMI, Figure 1) as a bismaleimide crosslinker to introduce disulfide (S-S) bridges between the PFMA brush chains. The S-S bonds can be cleaved (dissociate) upon thermal (40 °C) or photo (UV) stimulus and be regenerated through oxidation. Such reversible generation of the S-S bonds provides an alternative method to switch surface properties *via* crosslinking and decrosslinking. The photo-

responsive decrosslinking enabled spatial control in the crosslinked/decrosslinked areas using photomasks, yielding patterned brush surfaces with dual properties. In the present work, we combined the DA/rDA reactions and the S-S dissociation/regeneration to demonstrate wider applications. The reversible crosslinking, multi-responsiveness, high graft density, and metal-free preparation of the brush gels are attractive features in the present approach for creating functional surfaces.

EXPERIMENTAL SECTION

Preparation of Alkyl Iodide Initiator-Immobilized Silicon Wafer. A silicon wafer (8 mm × 8 mm) was cleaned with acetone (with sonication for 30 min), chloroform (with sonication for 30 min), and isopropanol (with sonication for 30 min). After drying under nitrogen flow, the wafer was placed in an ozone cleaner and radiated for 30 min. The wafer was immersed in a mixture of 6-(2-iodo-2-isobutyryloxy)-hexyltriethoxysilane (IHE, Figure 1), ethanol, and aqueous ammonia solution (1/89/10 (w/w/w)) at room temperature in a dark condition for one day. The wafer was washed with ethanol, sonicated in ethanol for 30 min, and dried under nitrogen flow to give an IHE-immobilized silicon wafer.

Surface-initiated Polymerization. The IHE-immobilized silicon wafer was immersed in a mixture of FMA (1.2 g , 7.2 mmol, 8000 mM), 2-iodo-2-methylpropionitrile (CP−I, Figure 1, 1.4 mg, 7.2 μmol, 8 mM), and tetra-*n*-octylammonium iodide (ONI, Figure 1, 34 mg, 0.058 mmol, 64 mM) in a Schlenk flask and heated at 60 °C under argon atmosphere with magnetic stirring for 6 h. The wafer was inclined to the wall of the Schlenk flask and the stir bar was located underneath the wafer. After the polymerization, the solution was cooled to room temperature. A

portion of the solution was diluted with tetrahydrofuran (THF) and analyzed with gel permeation chromatography (GPC) to determine the molecular weight of the free polymer (non-immobilized polymer formed from CP−I (non-immobilized alkyl iodide initiator)). It should be noted that the GPC was calibrated with standard poly(methyl methacrylate)s (PMMAs) and that the molecular weights determined with GPC were not absolute values but PMMA-calibrated values. Another portion of the solution was diluted with dimethyl sulfoxide-d_6 (DMSO-d_6) and analyzed with proton nuclear magnetic resonance (^{1}H NMR) to determine the monomer conversion. The wafer was washed with acetone and dried under nitrogen flow. The polymer brush was scratched for the measurement of the height gap between the scratched and unscratched areas by using an atomic force microscope (AFM). The brush thickness presented in all tables was subtracted by the thickness of the IHE initiator layer (2 nm). The number-average molecular weight (M_n), polymer dispersity ($Đ = M_w/M_n$, where M_w is the weight-average molecular weight) of the free polymer, and the dry thickness (h) of the polymer brush are summarized in Table 1. For determining the thickness of the swollen polymer brush, we placed the wafer with the polymer brush in toluene for 30 min. The wet wafer (the swollen polymer brush covered with the solvent layer) was analyzed with AFM shortly before drying.

General Crosslinking Procedure of PFMA Brushes. The wafer with the PFMA brush was immersed in a mixture of a crosslinker (1wt% for DIMI or 0.5wt% for DSMI) and DMF (1.5 g (99wt%) for DIMI and 1.0 g (99.5wt%) for DSMI) in a Schlenk flask and heated at 70 °C under argon atmosphere with magnetic stirring for 14 h. The wafer was cleaned by ultra-sonication in acetone for 30 min and dried under nitrogen flow.

General Thermal Decrosslinking Procedure of Crosslinked PFMA Brushes. The wafer with the crosslinked PFMA brush was immersed in a mixture of a crosslinker trap (FMA (5wt%)

or 2-furyl methyl ketone (5wt%)) and DMF (1.5 g (95wt%) for FMA and 2.0 g (95wt%) for 2-furyl methyl ketone) in a Schlenk flask and heated at 110 °C with magnetic stirring for 14 h. The wafer was cleaned by ultra-sonication in acetone for 30 min and dried under nitrogen flow.

Calculation of Graft Density and Surface Occupancy.[23,24] As mentioned, the M_n values determined with GPC were not absolute values but PMMA-calibrated values. Therefore, in the present work, we estimated the degree of polymerization (DP) of the polymer from the $[monomer]_0/[CP{-}I]_0$ ratio multiplied by the monomer conversion during the polymerization (DP = $([monomer]_0/[CP{-}I]_0)\times$(monomer conversion)). This estimate is not strictly accurate but would be viewed as a good approximation.

The graft density (σ) of the polymer brush was calculated using the estimated DP value and the dry thickness (h) of the polymer brush according to equation (1):

$$\sigma = \frac{h\rho N_A}{\mathrm{DP} \times (\text{molecular weight of monomer})} \quad (1)$$

where ρ is the polymer density, N_A is the Avogadro's number, and DP × (molecular weight of monomer) is the estimated molecular weight of the polymer. The polymer density of PFMA is 1.26 g/mL (in bulk).[53] The polymer density of poly(2-hydroxyethyl methacrylate) (PHEMA) is 1.15 g/mL (in bulk).[54]

The surface occupancy (σ^*) of the polymer brush was calculated using the estimated DP value and the h value according to equation (2):

$$\sigma^* = \frac{h}{0.25\ \text{nm} \times \text{DP}} \times 100\ (\%) \qquad (2)$$

where the length of a repeating unit in the polymer was assumed to be 0.25 nm.

Calculation of Surface Free Energy.[55,56] The surface energy (solid-vapor surface tension) (γ_S) of the polymer brush was obtained by measuring the water and diiodomethane contact angles and by using Owens-Wendt (extended Fowkes') equations (3)−(5):

$$(1 + \cos\theta)\gamma_L = 2\sqrt{\gamma_S^d \gamma_L^d} + 2\sqrt{\gamma_S^p \gamma_L^p} \qquad (3)$$

$$\gamma_L = \gamma_L^d + \gamma_L^p \qquad (4)$$

$$\gamma_S = \gamma_S^d + \gamma_S^p \qquad (5)$$

where θ is the contact angle, γ_L is the liquid-vapor surface tension, γ_L^d and γ_L^p are the liquid-vapor surface tensions of the dispersive and polar components, respectively, and γ_S^d and γ_S^p are the solid-vapor surface tensions of the dispersive and polar components, respectively. The surface tension values of the liquids used for calculation were γ_L^d(water) = 21.8 mJ/m^2, γ_L^p(water) = 51.0 mJ/m^2, γ_L^d(diiodomethane) = 48.5 mJ/m^2, and γ_L^p(diiodomethane) = 2.3 mJ/m^2. Equation (3) is valid when there is no surface pressure. In the presence of surface pressure, the obtained γ_S value will be an apparent value.

RESULTS AND DISCUSSION

DA and rDA Reactions of FMA and PFMA in Solution. Before studying the polymer brushes, we studied the DA reaction between the FMA monomer (0.56 M, 20 eq) and DIMI (0.028 M, 1 eq) in DMSO-d_6 at 60 °C (in solution). After 8 h, ^{1}H NMR spectroscopy (Supporting Information, Figure S2) showed the disappearance of the maleimide (DIMI) (a signal at 7.16 ppm for CH=CH) and the generation of the DA adduct (signals at 6.55, 5.25, and 3.25−3.18 ppm for the [2+4] cycloaddition moiety), suggesting the successful DA reaction between FMA and DIMI. Instead of the FMA monomer, we also studied the PFMA polymer (M_n = 24000 and $Đ$ = 1.35 (PMMA-calibrated GPC values)). PFMA (49.75wt%, monomer unit = 2.8 M, 210 eq) was reacted with DIMI (0.5wt%, 0.013 M, 1 eq) in DMF (49.75wt%) at 70 °C (Figure 2a). PFMA was converted to the crosslinked PFMA gel after 14 h, confirming the occurrence of the DA crosslinking of PFMA with DIMI. The crosslinked PFMA gel was decrosslinked at 110 °C *via* a rDA reaction. In the decrosslinking, the FMA monomer was added to trap the released DIMI. The above obtained crosslinked PFMA gel swollen in DMF (50wt%), the FMA monomer (2.5wt%, 25 eq to DIMI), and additional DMF (47.5wt%) were heated at 110 °C for 24 h. After the decrosslinking, the gel was reverted to a liquid state (Figure 2a). Figure 2b shows the GPC chromatograms of the original PFMA (black line) and the decrosslinked PFMA (red line), suggesting that a large fraction of the decrosslinked PFMA was reverted to the original PFMA. A shoulder peak was observed on the high-molecular-weight side for the decrosslinked PFMA and was attributed to the remaining coupled PFMA chains, which were not able to completely be eliminated after heating at 110 °C for 24 h. The M_n value (28000) of the decrosslinked PFMA was relatively close to that (24000) of the original PFMA, suggesting, with respect to the number average, a large fraction of the polymer was reverted to the original PFMA. These results

indicate that the DA and rDA reactions between PFMA and DIMI was highly effective for the reversible crosslinking of PFMA. It should be noted that the full (100%) decrosslinking via the rDA reaction was difficult to achieve. For the polymer brushes described below, after the rDA reaction, the brushes might still be partially crosslinked to small degrees. In a strict sense, the reversible crosslinking-decrosslinking via the DA and rDA reactions described below is viewed as nearly reversible crosslinking-decrosslinking.

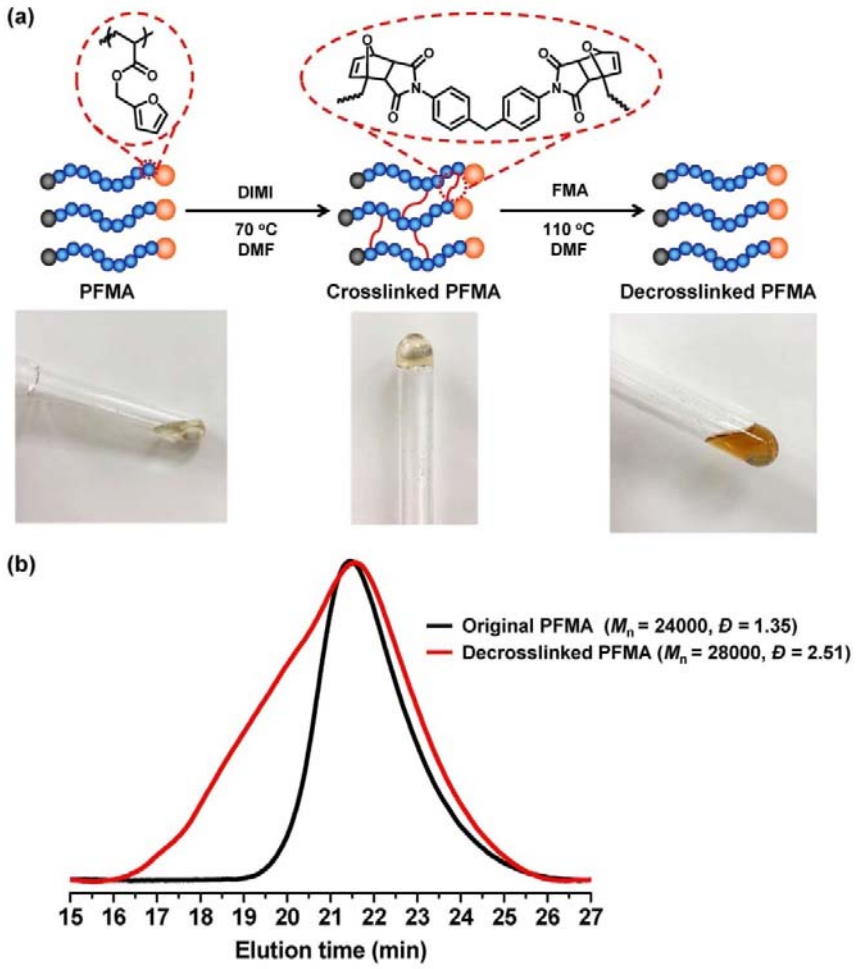

Figure 2. (a) Schematic illustration and images of the uncrosslinked, crosslinked, and decrosslinked PFMA. (b) GPC chromatograms of original (uncrosslinked) PFMA (black line) and decrosslinked PFMA (red line).

Table 1. Synthesis of Concentrated PFMA and Copolymer Brushes.[a]

Entry	M_1[b]	M_2[c]	$[M_1]_0/[M_2]_0/[CP-I]_0/[ONI]_0$ (mM)[d]	Conv of M_1/M_2 (%)[e]	M_n[f] ($M_{n,theo}$[g])	$Đ$[f]	DP[h]	h (nm)	σ (chains /nm^2)	σ^* (%)
1	FMA	−	8000/0/8/64	13/−	21000 (21000)	1.35	130	10	0.35	31
2	FMA	PFPMA	4000/4000/8/64	7/14	21000 (21000)	1.41	105	7	0.25[i]	27
3	FMA	HEMA	4000/4000/8/64	6/9	23000 (11000)	1.49	75	5	0.16	27

[a]Polymerizations were perform at 60 °C for 6 h (entry 1), 8 h (entry 2) and 24 h (entry 3). [b]FMA monomer. [c]Comonomer. [d]The target DP at a full (100%) monomer conversion was 1000. [e]Monomer conversion determined with ^{1}H NMR. [f]PMMA-calibrated THF-GPC values of the free polymers for entries 1 and 2. PMMA-calibrated DMF-GPC value of the free polymer for entry 3. [g]Theoretical M_n calculated with $[M_1]_0$, $[M_2]_0$, $[CP-I]_0$, and monomer conversion. [h]Estimated DP values according to DP = ($[monomer]_0/[CP-I]_0$)×(monomer conversion). [i]Assuming the density of PFPMA (polymer) is the same as that of PFMA (monomer) (= 1.26 g/mL).

Synthesis of Polymer Brushes. Table 1 (entry 1) shows the synthetic result of the homo-PFMA brush. An alkyl iodide initiator IHE (Figure 1) was immobilized on a silicon-wafer (Scheme 2). The IHE-immobilized wafer was heated in a mixture of FMA (8000 mM, 1000 eq), CP−I (Figure 1, 8 mM, 1 eq) as a non-immobilized (free) alkyl iodide initiator, and ONI (Figure 1, 64 mM, 8 eq) as a catalyst at 60 °C for 6 h, yielding the PFMA brush (Scheme 2). The free initiator (CP−I) was added because its addition can improve the control over M_n and dispersity, and the M_n and $Đ$ values of the free polymer generated from the free initiator are in good agreement with those of the graft polymer in many cases. The obtained free PFMA had M_n = 21000 and $Đ$ = 1.35 (PMMA-calibrated GPC values). The dry thickness (h) of the PFMA brush was 10 nm. Because the M_n value determined with GPC was not an absolute value, we estimated the DP of the polymer from the $[monomer]_0/[CP-I]_0$ ratio multiplied by the monomer conversion (DP = ($[monomer]_0/[CP-I]_0$)×(monomer conversion)). Using this DP value and assuming an identical M_n value for the graft and free polymers, the σ and σ* values were calculated to 0.35 chains/nm^2 and 31%, respectively.

Random copolymerizations of FMA with hydrophobic 2,2,3,3,3-pentafluoropropyl methacrylate (PFPMA) and hydrophilic 2-hydroxyethyl methacrylate (HEMA) yielded PFMA-*r*-PPFPMA and PFMA-*r*-PHEMA random copolymer brushes with higher hydrophobicity and higher hydrophilicity, respectively (Table 1, entries 2 and 3), where PPFPMA is poly(2,2,3,3,3-pentafluoropropyl methacrylate) and PHEMA is poly(2-hydroxyethyl methacrylate). The M_n and $Đ$ values of the obtained free copolymers were 21000−23000 and 1.41−1.49, respectively (PMMA-calibrated GPC values). The graft densities were high (σ = 0.16−0.25 chains/nm^2 and σ^* = 27%) and located in a concentrated brush regime ($\sigma^* \geq 10\%$). In the present work, we intentionally stopped the polymerizations at low monomer conversions (6−13%) of FMA to prevent the self-crosslinking reaction of the FMA units.[57]

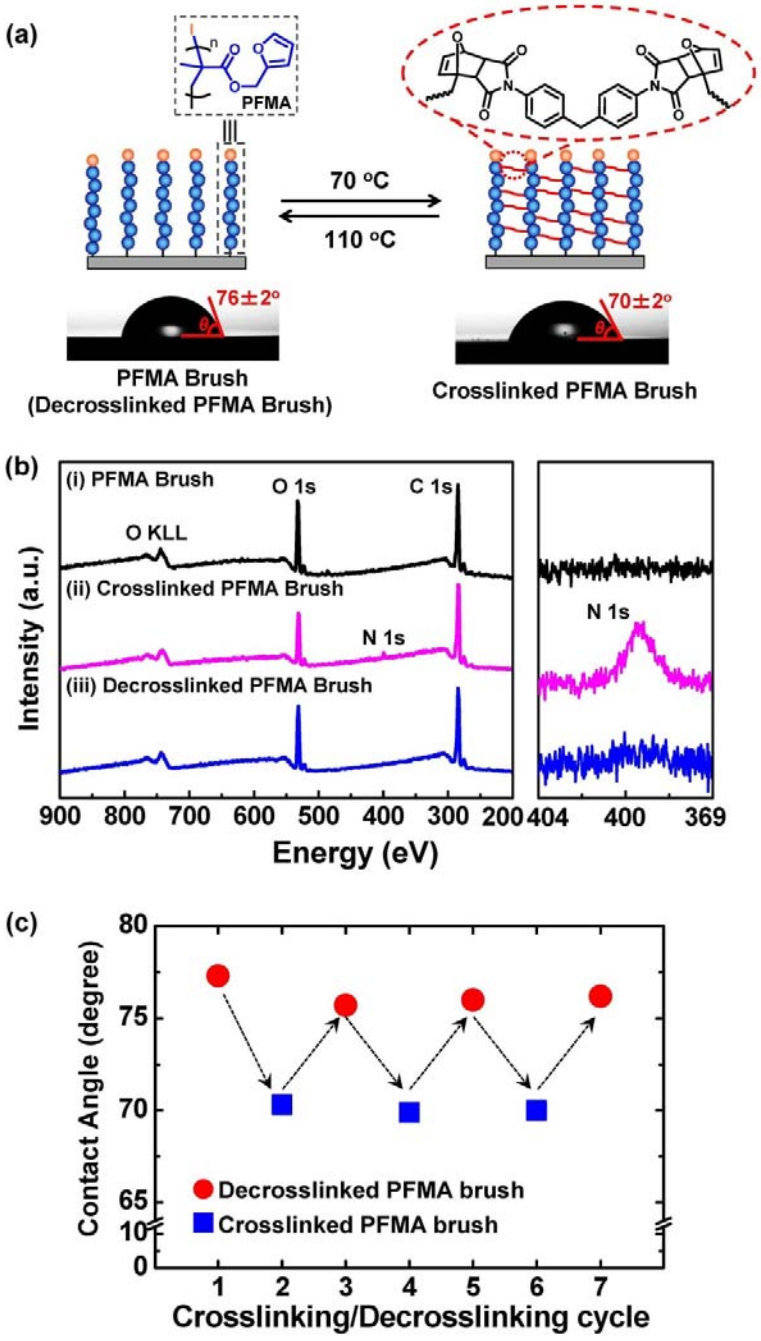

Figure 3. (a) Reversible crosslinking (70 ^{o}C) and decrosslinking (110 ^{o}C) of PFMA brush via DA and rDA reactions using DIMI crosslinker and WCA analysis. The WCA analysis (76^{o}) for PFMA brush (left) is not for the original PFMA brush but for the decrosslinked PFMA brush generated from the crosslinked PFMA brush. (b) XPS survey and high resolution N 1s spectra of PFMA brushes. (c) Change in WCA by crosslinking and decrosslinking of PFMA brush in a cycled manner.

Reversible Thermal Crosslinking and Decrosslinking of PFMA Brushes. The obtained brushes were crosslinked with DIMI *via* the DA reaction (Figure 3a). The wafer with the homo-PFMA brush (Table 1, entry 1) was immersed in a DMF solution with DIMI (1wt%) and heated at 70 °C to crosslink the brush chains. Figures 3b shows the X-ray photoelectron spectroscopy (XPS) analysis of the uncrosslinked PFMA and crosslinked PFMA brushes. In the spectrum of the crosslinked PFMA brush, the nitrogen 1s electron signal (399 eV) originated from DIMI was clearly observed, while no nitrogen signal was detected for the uncrosslinked PFMA brush. We also investigated the swelling behaviors of the uncrosslinked and crosslinked PFMA brushes. In the dry state, the uncrosslinked and crosslinked brushes similarly had 10 nm in thickness. If all FMA units are crosslinked through DIMI (crosslinker), the dry thickness should increase from 10 nm (no crosslinking) to 21 nm (full crosslinking), considering the molecular weights of FMA and DIMI. The observed similar thickness (10 ± 1 nm) suggests that the extent of crosslinking is < 9% (= 1 nm/(21–10 nm)). This relatively small value (< 9%) would be reasonable because the studied polymer brush is a concentrated one (σ^* = 31%) and the conformation of the polymer chains (hence the gel thickness) is fixed at even a small extent of crosslinking. After swelling in toluene, the thicknesses of the uncrosslinked and crosslinked brushes increased to 19 nm and 12 nm, respectively. The smaller increase for the crosslinked brush is reasonable, because the brush chains can not freely extend due to the crosslinking among the chains. Thus, the XPS and swelling analyses show the occurrence of the crosslinking DA reaction between the PFMA brush chains and DIMI.

Table 2. Contact Angles (CA) and Apparent Solid-Vapor Surface Tensions (γ_S) of Polymer Brushes.

Entry	Polymer Brush[a]	Uncrosslinked			Crosslinked		
		CA (°) (Water)	CA(°) (CH_2I_2)	γ_S (mJ/m^2)	CA (°) (Water)	CA(°) (CH_2I_2)	γ_S (mJ/m^2)
1	PFMA	77	31	44.4	70	16	50.0
2	PFMA-*r*-PPFPMA	90	53	32.7	85	43	38.2
3	PFMA-*r*-PHEMA	65	34	46.8	54	27	53.6

[a]The synthetic conditions and characterization of the polymer brushes are given in Table 1.

The static water contact angle (WCA) of the uncrosslinked PFMA brush was 77° and that of the crosslinked PFMA brush was 70° (Figure 3a and Table 2, entry 1). In the field of polymer brushes, a decreased WCA by crosslinking was first experimentally observed in poly(acrylamide) brush systems by Schönherr and Spencer[58] and later on in other systems.[27] A brush polymer anchors on the solid substrate at one chain end and can bridge to the liquid-vapor interface at the other chain end during the WCA analysis. Leermakers *et al.* suggested that the bridging of the polymer chain to the liquid-vapor interface can generate surface pressure (internal pressure inside the brush) and hence increase the WCA.[59] Schönherr and Spencer suggested that the lateral cross-linking of polymer brush chains can decrease the chain conformational freedom, hence inhibiting the bridging effect and decreasing the WCA.[58] We observed the decrease in the WCA after the DA reaction (Figure 3a and Table 2, entry 1), which supports the formation of the crosslinked polymer brush. However, it should be noted that DIMI (used as a crosslinker) is slightly more hydrophilic (due to the presence of imide) than PFMA and that the incorporation of DIMI in the brush layer might also contribute to the decrease in the WCA.

Exploiting the reversibility of the DA reaction, the crosslinked PFMA brush was decrosslinked with the addition of the FMA monomer (as a trap of DIMI) at 110 °C *via* the rDA

reaction. After the rDA reaction, the WCA was restored to 76° (Figure 3a). The XPS spectrum of the decrosslinked PFMA brush showed no nitrogen 1s signal of DIMI (Figure 3b), meaning the successful decrosslinking. 2-Furyl methyl ketone, which is a furan derivative obtainable from plant biomass, was also able to use as a trap of DIMI in the rDA reaction. The DA and rDA reactions of PFMA and DIMI were reversible and repeatable for several cycles. Figure 3c shows that the WCA was consistently sustained at approximate 77° and 70° for the decrosslinked and crosslinked PFMA brushes, respectively.

The PFMA-*r*-PPFPMA and PFMA-*r*-PHEMA brushes are more hydrophobic and more hydrophilic than the PFMA brush and showed the WCA values of 90° and 65°, respectively (Table 2, entries 2 and 3). After the crosslinking with DIMI, the WCA value decreased to 85° and 54°, respectively (Table 2, entries 2 and 3). The change in the cosine of WCA tended to increase in the order of the most hydrophobic PFMA-*r*-PPFPMA brush (cos(85°) – cos(90°) = 0.087), pure PFMA brush (cos(70°) – cos(77°) = 0.117), and the most hydrophilic PFMA-*r*-PHEMA brush (cos(54°) – cos(65°) = 0.165). This result suggests that the change in the surface pressure by the crosslinking became more significant in this order. A hydrophobic brush is not much swollen with water and would not effectively bridge to the liquid-vapor interface even in the non-crosslinked state. Therefore, the inhibition of the bridging effect by the crosslinking would be marginal.[27] In contrast, a hydrophilic brush is swollen with water and would effectively bridge to the liquid-vapor interface without the crosslinking. The crosslinking would significantly inhibit the bridging effect and give a smaller WCA. The decrosslinking of the crosslinked PFMA-*r*-PPFPMA and PFMA-*r*-PHEMA brushes was also achieved at 110 °C. These results demonstrate that the DA and rDA reactions are applicable for PFMA-based brushes with different comonomers (different hydrophobicity).

In addition, the apparent solid-vapor surface tension (γ_S) was determined for the uncrosslinked and crosslinked brushes by measuring the contact angles using water and diiodomethane (CH_2I_2) droplets and by using equations (3)–(5). The results are summarized in Table 2. The γ_S value increased by the crosslinking from 44.4 mJ/m^2 to 50.0 mJ/m^2 for PFMA, from 32.7 mJ/m^2 to 38.2 mJ/m^2 for PFMA-*r*-PPFPMA, and from 46.8 mJ/m^2 to 53.6 mJ/m^2 for PFMA-*r*-PHEMA. Thus, the surface wettability was able to be modulated *via* the crosslinking and decrosslinking of the brushes and the use of hydrophilic and hydrophobic comonomers.

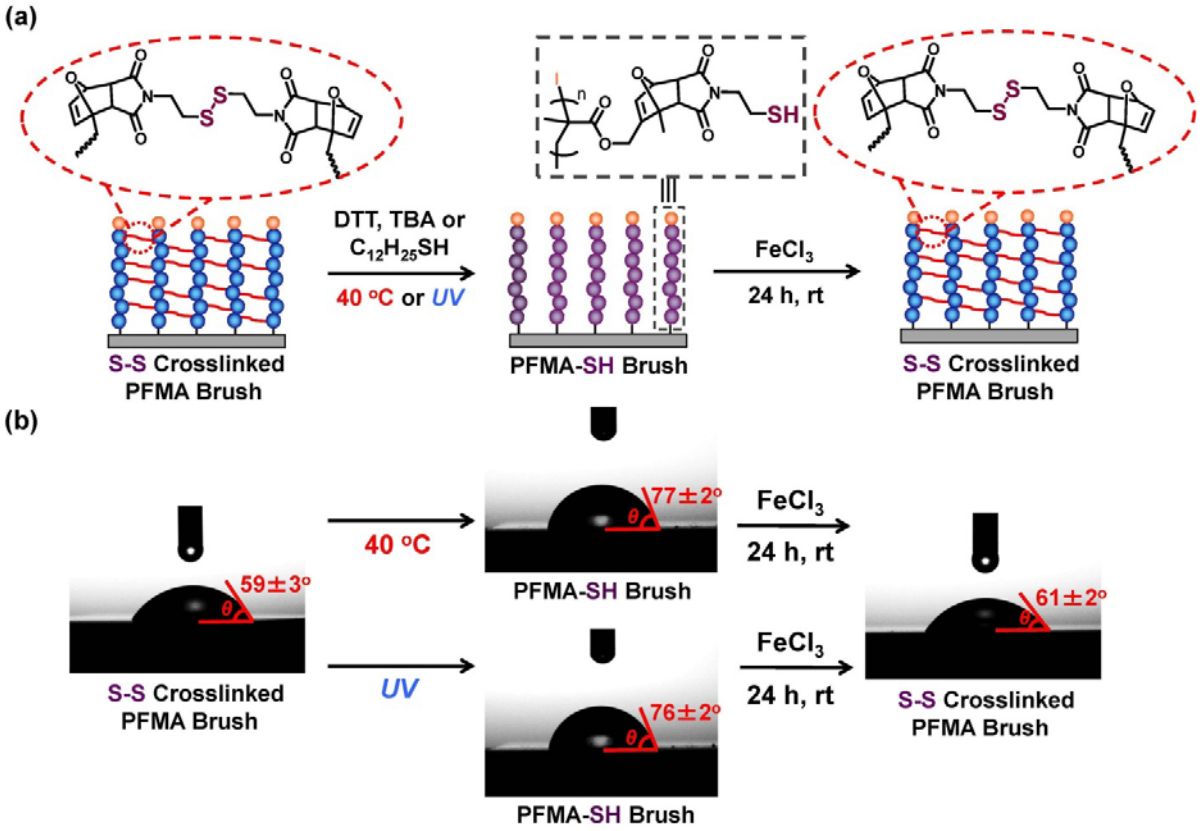

Figure 4. (a) S-S crosslinked PFMA brush, decrosslinked PFMA-SH brush generated via thermal- or photo-stimuli, and S-S recrosslinked brush generated via oxidative SH coupling. (b) WCA analysis of S-S crosslinked PFMA brush, decrosslinked PFMA-SH brush, and S-S recrosslinked brush.

Photo- and Redox-Responsive Polymer Brushes. Instead of DIMI, DSMI was used as a functional crosslinker with a disulfide (S-S) bond. The PFMA brush was crosslinked with DSMI *via* the DA reaction at 70 °C to give a disulfide-bond crosslinked PFMA (S-S crosslinked PFMA) brush (Figure 4a). The WCA of the S-S crosslinked PFMA brush was 59° (Figure 4b), which is smaller than that of the DIMI-crosslinked PFMA brush, because the diethyl disulfide group in DSMI is more hydrophilic than the diphenylmethane group in DIMI.

The S-S bond of the S-S crosslinked PFMA brush was able to reversibly be cleaved and regenerated through reduction-oxidation reactions. For the reduction (S-S dissociation), we used a thermal or photo stimulus under a mild condition (40 °C or UV light). The wafer with the S-S crosslinked PFMA brush was heated in a DMF solution of dithiothreitol (DTT, 5wt%) or tributylamine (TBA, 5wt%) as a reducing agent at 40 °C for 10 h (Figure 4b) or was irradiated in a DMF solution containing a photo-initiator (Irgacure D-2959) and either DTT or TBA under a UV light (365 nm, 900 mW/cm^2) for 30 min (Figure 4b). The S-S bond was converted to thiols, generating a decrosslinked thiol-functionalized PFMA (PFMA-SH) brush (Figure 4a). The WCA of the S-S crosslinked PFMA brush was 59°, as mentioned above, and those of the decrosslinked PFMA-SH brushes increased to 76°–77°. The increase in the WCA indicates higher surface pressures and the successful decrosslinking of the brushes via the thermal and photo-irradiation treatments. The use of DTT and TBA gave the same results (the same WCA). The S-S bond was slowly cleaved in the presence of TBA even without the heating at 40 °C or the UV irradiation.[60] At room temperature, the WCA increased from 59° to 63° for 30 min and to 67° for 10 h. The heating and the UV irradiation were effective to accelerate the S-S bond cleavage reaction. Instead of DTT and TBA, 1-dodecanethiol ($C_{12}H_{25}SH$, 25wt%) was also successfully used to decrosslink the S-S crosslinked PFMA brush. The obtained PFMA-SH brushes were able to be

crosslinked again *via* an oxidative coupling of thiols using iron(III) chloride in a mild condition (room temperature for 24 h). After the re-crosslinking, the WCA was recovered to 61°, which is close to that (59°) of the original S-S crosslinked PFMA brush. This result demonstrates the stimuli-responsive crosslinking and decrosslinking of the S-S crosslinked PFMA brush.

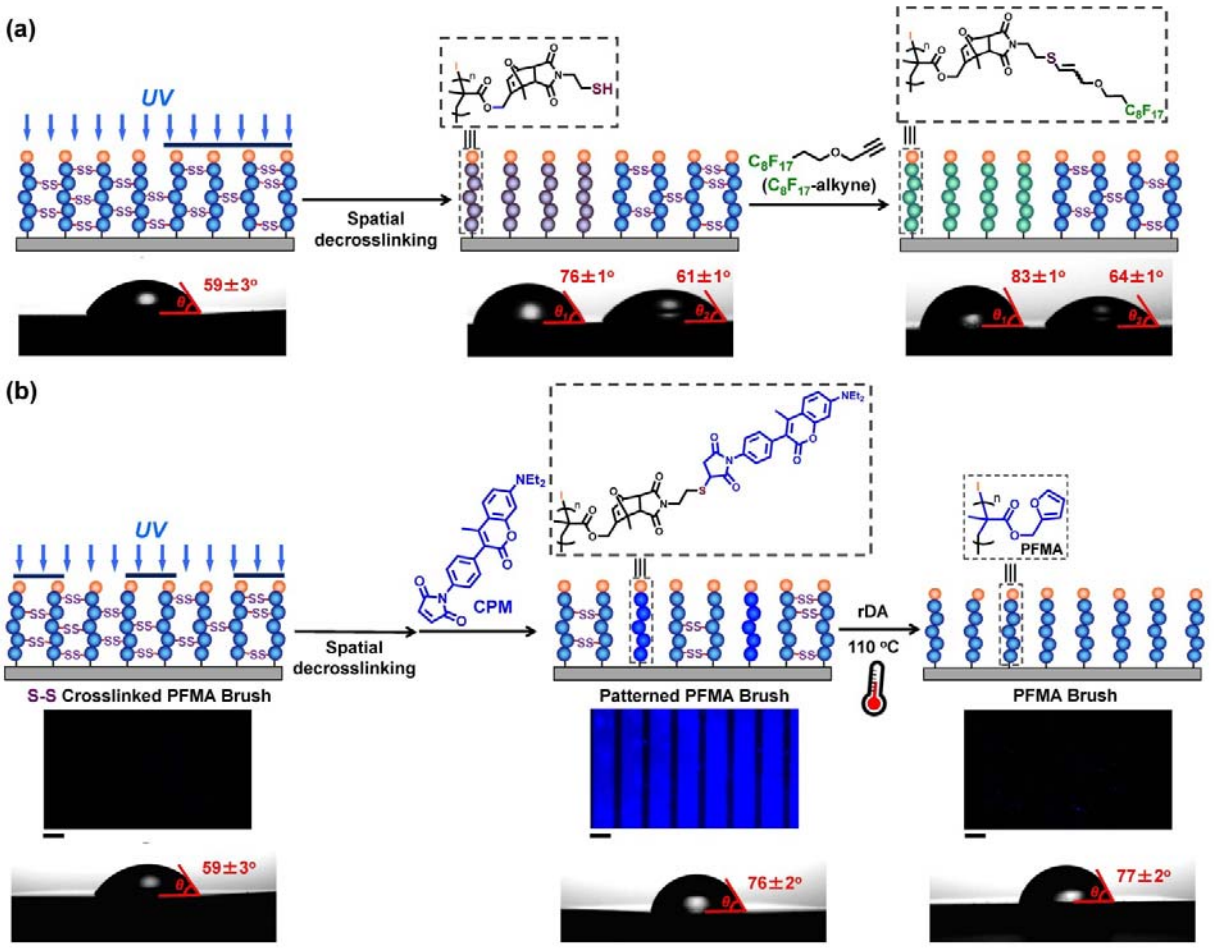

Figure 5. (a) Synthesis and WCA analysis of binary patterned PFMA brushes. (b) A sequence of drawing, labeling (CPM fluorophore labeling), and erasure of the brush pattern on a single surface, fluorescence microscope images, and WCA analysis. The scale bar indicates 50 μm in the fluorescence microscope images.

Spatial Control of Functional Polymer Brushes. Spatially controlled (patterned) polymer brushes have attracted attention towards various applications to, *e.g.*, bio-microarrays, optoelectronic interfaces, and microfluidic systems.[61−67] Exploiting the photo-responsive S-S cleavage demonstrated above, we spatially decrosslink the S-S crosslinked PFMA brush and created a binary patterned brush with crosslinked and decrosslinked areas. A uniform S-S crosslinked PFMA brush was prepared first, subsequently a half of the surface was covered with a clean silicon wafer, and the surface was irradiated by UV light (Figure 5a). The unmasked area was converted to a decrosslinked PFMA-SH brush, generating a binary patterned brush with two different WCAs of 76° for the decrosslinked PFMA-SH brush and 61° for the unreacted S-S crosslinked PFMA brush (Figure 5a). The PFMA-SH brush further reacted with 3-((2-perfluorooctyl)ethoxy)propyne (C_8F_{17}-alkyne, Supporting Information) through a thiol-yne addition. The perfluorinated moiety was successfully attached on the PFMA-SH brushes, increasing the WCA to 83° (Figure 5a). Thus, the binary patterned surface with tailored hydrophobicity and hydrophilicity was successfully obtained. Meanwhile, the S-S bond slowly dissociated during the WCA analysis due to the light irradiation for imaging, resulting in the slight increase in the WCA from 59° to 64° for the S-S crosslinked PFMA brush area (Figure 5a).

The spatial decrosslinking also offered a striped patterned PFMA brush. The use of a striped photomask (with masked 25 μm and unmasked 50 μm pitches (Figure S1)) led to a patterned brush with the S-S crosslinked PFMA and decrosslinked PFMA-SH domains after the UV irradiation (Figure 5b). The PFMA-SH domain was subsequently labelled with a fluorophore-containing maleimide, 7-diethylamino-3-(4-maleimidophenyl)-4-methylcoumarin (CPM), though thiol–maleimide Michael addition (Figure 5b). The fluorescence microscopy image shows a clear striped pattern, demonstrating the successful decrosslinking of the S-S crosslinked PFMA brush

and subsequent functionalization of the brush in a patterned manner. The obtained patterned brush was heated in a DMF solution of FMA (as a trap of the maleimides) at 110 °C and underwent the rDA reaction (Figure 5b). Both the fluorophore (CPM) and the crosslinker (DSMI), which were linked to the PFMA brush, were released from the PFMA brush via the rDA reaction, recovering the original uniform uncrosslinked PFMA brush. (The WCA (77°) of the recovered brush (Figure 5b) was identical to that (77°) of the original PFMA brush (Table 2, entry 1).) (In Figure 5b, the similarity of the WCA (76°) of the patterned PFMA brush to that of the recovered PFMA brush (77°) would be coincidence.) Therefore, combining the DA reaction, the photo-patterning, the SH functionalization, and the rDA reaction, we were able to draw, label, and erase the brush pattern on a single surface, which is a unique feature of the present approach.

CONCLUSIONS

The concentrated PFMA brushes were crosslinked in the presence of the bismaleimide crosslinkers at 70 °C *via* the DA reaction and decrosslinked at 110 °C *via* the rDA reaction, offering the temperature-responsive reversible PFMA brush gels. The wettability of the PFMA brush was tuned by the crosslinking and decrosslinking and the use of hydrophobic and hydrophilic comonomers in the PFMA brush. The use of the DSMI crosslinker further provided the S-S bond at the crosslinking point. The S-S bond was cleaved and regenerated by the reductive and oxidative stimuli, respectively, offering another decrosslinking/crosslinking pathway. Using the photo-induced reduction, the binary and striped patterned brushes with the crosslinked and decrosslinked domains were obtained. The combination of the DA/rDA reaction with the reversible S-S bond cleavage offered multi-responsive brush gels, *e.g.*, enabling a sequence of drawing, labeling, and erasure of the brush gel pattern on a single surface. The

reversible crosslinking, multi-responsiveness, access to patterned structures, and metal-free synthetic procedure are attractive features of the present approach. The applications on the modulation of surface wettability, surface patterning, rewritable surface, and spatial fluorescence labeling demonstrated in the present work may be exploited for adsorptive/desorptive interfaces, rewritable interfaces, and molecular recognition and sensing interfaces, for example.

ASSOCIATED CONTENT

Supporting Information. The Supporting Information is available free of charge on the ACS Publications website at http://pubs.acs.org. Materials and instrument, DA and rDA reactions of FMA and PFMA, synthesis and crosslinking/decrosslinking of polymer brushes, synthesis of C_8F_{17}-alkyne, and XPS data.

AUTHOR INFORMATION

Corresponding Author

*E-mail: agoto@ntu.edu.sg

Author Contributions

‡These authors contributed equally. (X. M. Sim and C.-G. Wang)

ORCID

C.-G Wang: 0000-0001-6986-3961

A. Goto: 0000-0001-7643-3169

Notes

The authors declare no competing financial interest.

ACKNOWLEDGMENT

This work was supported by National Research Foundation (NRF) Singapore under NRF Investigatorship (NRF-NRFI05-2019-0001) and Ministry of Education, Singapore, under Academic Research Fund (AcRF) Tier 2 (MOE2017-T2-1-018).

REFERENCES

(1) Mendes, P. M. Stimuli-Responsive Surfaces for Bio-applications. *Chem. Soc. Rev.* **2008**, *37*, 2512−2529.

(2) Yang, H.; Yuan, B.; Zhang, X. Supramolecular Chemistry at Interfaces: Host−Guest Interactions for Fabricating Multifunctional Biointerfaces. *Acc. Chem. Res.* **2014**, *47*, 2106−2115.

(3) Su, B.; Tian, Y.; Jiang, L. Bioinspired Interfaces with Superwettability: From Materials to Chemistry. *J. Am. Chem. Soc.* **2016**, *138*, 1727−1748.

(4) Gupta, R. K.; Dunderdale, G. J.; England, M. W.; Hozumi, A. Oil/Water Separation Techniques: a Review of Recent Progresses and Future Directions. *J. Mater. Chem. A* **2017**, *5*, 16025−16058.

(5) Keating IV, J. J.; Imbrogno, J.; Belfort, G. Polymer Brushes for Membrane Separations: A Review. *ACS Appl. Mater. Interfaces* **2016**, *8*, 28383−28399.

(6) Zoppe, J. O.; Ataman, N. C.; Mocny, P.; Wang, J.; Moraes, J.; Klok, H.-A. Surface-Initiated Controlled Radical Polymerization: State-of-the-Art, Opportunities, and Challenges in Surface and Interface Engineering with Polymer Brushes. *Chem. Rev.* **2017**, *117*, 1105−1318.

(7) Chen, W.-L.; Cordero, R.; Tran, H.; Ober, C. K. 50th Anniversary Perspective: Polymer Brushes: Novel Surfaces for Future Materials. *Macromolecules* **2017**, *50*, 4089−4113.

(8) Wu, J.-G.; Chen, J.-H.; Liu, K.-T.; Luo, S.-C. Engineering Antifouling Conducting Polymers for Modern Biomedical Applications. *ACS Appl. Mater. Interfaces* **2019**, *11*, 21294−21307.

(9) Ma, S.; Zhang, X.; Yu, B.; Zhou, F. Brushing up Functional Materials. *NPG Asia Mater.* **2019**, *11*, 24.

(10) Stuart, M. A. C.; Huck, W. T. S.; Genzer, J.; Muller, M.; Ober, C.; Stamm, M.; Sukhorukov, G. B.; Szleifer, I.; Tsukruk, V. V.; Urban, M.; Winnik, F.; Zauscher, S.; Luzinov, I.; Minko, S. Emerging Applications of Stimuli-Responsive Polymer Materials. *Nat. Mater.* **2010**, *9*, 101−113.

(11) Chen, T.; Ferris, R.; Zhang, J.; Ducker, R.; Zauscher, S. Stimulus-responsive Polymer Brushes on Surfaces: Transduction Mechanisms and Applications. *Prog. Polym. Sci.* **2010**, *35*, 94−112.

(12) Li, B.; Yu, B.; Ye, Q.; Zhou, F. Tapping the Potential of Polymer Brushes through Synthesis. *Acc. Chem. Res.* **2015**, *48*, 229−237.

(13) Hirai, T.; Kobayashi, M.; Takahara, A. Control of the Primary and Secondary Structure of Polymer Brushes by Surface-Initiated Living/Controlled Polymerization. *Polym. Chem.* **2017**, *8*, 5456−5468.

(14) Badoux, M.; Billing, M.; Klok, H.-A. Polymer Brush Interfaces for Protein Biosensing Prepared by Surface-Initiated Controlled Radical Polymerization. *Polym. Chem.* **2019**, *10*, 2925−2951.

(15) Goto, A.; Ohtsuki, A.; Ohfuji, H.; Tanishima, M.; Kaji, H. Reversible Generation of a Carbon-centered Radical from Alkyl Iodide Using Organic Salts and their Application as Organic Catalysts in Living Radical Polymerization. *J. Am. Chem. Soc.* **2013**, *135*, 11131−11139.

(16) Ohtsuki, A.; Lei, L.; Tanishima, M.; Goto, A.; Kaji, H. Photocontrolled Organocatalyzed Living Radical Polymerization Feasible over a Wide Range of Wavelengths. *J. Am. Chem. Soc.* **2015**, *137*, 5610−5617.

(17) Wang, C.-G.; Goto, A. Solvent-Selective Reactions of Alkyl Iodide with Sodium Azide for Radical Generation and Azide Substitution and Their Application to One-Pot Synthesis of Chain-End-Functionalized Polymers. *J. Am. Chem. Soc.* **2017**, *139*, 10551−10560.

(18) Liu, X.; Wang, C.-G.; Goto, A. Polymer Dispersity Control by Organocatalyzed Living Radical Polymerization. *Angew. Chem. Int. Ed.* **2019**, *58*, 5598−5603.

(19) Xu, H.; Wang, C.-G.; Lu, Y.; Goto, A. Pyridine *N*-Oxide Catalyzed Living Radical Polymerization of Methacrylates *via* Halogen Bonding Catalysis. *Macromolecules* **2019**, *52*, 2156−2163.

(20) Wang, C.-G.; Oh, X. Y.; Liu, X.; Goto, A. Self-Catalyzed Living Radical Polymerization Using Quaternary-Ammonium-Iodide-Containing Monomers. *Macromolecules* **2019**, *52*, 2712−2718.

(21) Mao, W.; Wang, C.-G.; Lu, Y.; Faustinelie, W.; Goto, A. Carboxylate, Nitrate, Sulfonate, and Phosphate Catalysts for Living Radical Polymerization *via* Oxygen–Iodine Halogen Bonding Catalysis. *Polym. Chem.* **2020**, *11*, 53−60.

(22) Wang, C.-G.; Chang, J. J.; Foo, E. Y. J.; Niino, H.; Chatani, S.; Hsu, S. Y.; Goto, A. Recyclable Solid-Supported Catalysts for Quaternary Ammonium Iodide-Catalyzed Living Radical Polymerization. *Macromolecules* **2020**, *53*, 51−58.

(23) Wang, C.-G.; Chen, C.; Sakakibara, K.; Tsujii, Y.; Goto, A. Facile Fabrication of Concentrated Polymer Brushes with Complex Patterning by Photocontrolled Organocatalyzed Living Radical Polymerization. *Angew. Chem. Int. Ed.* **2018**, *57*, 13504−13508.

(24) Wang, C.-G.; Yong, H. W.; Goto, A. Effective Synthesis of Patterned Polymer Brushes with Tailored Multiple Graft Densities. *ACS Appl. Mater. Interfaces* **2019**, *11*, 14478−14484.

(25) Tsujii, Y.; Ohno, K.; Yamamoto, S.; Goto, A.; Fukuda, T. Structure and Properties of High-Density Polymer Brushes Prepared by Surface-Initiated Living Radical Polymerization. *Adv. Polym. Sci.* **2006**, *197*, 1−45.

(26) Huang, W.; Baker, G. L.; Bruening, M. L. Controlled Synthesis of Cross-Linked Ultrathin Polymer Films by Using Surface-Initiated Atom Transfer Radical Polymerization. *Angew. Chem. Int. Ed.* **2001**, *40*, 1510−1512.

(27) Dehghani, E. S.; Spencer, N. D.; Ramakrishna, S. N.; Benetti, E. M. Crosslinking Polymer Brushes with Ethylene Glycol-Containing Segments: Influence on Physicochemical and Antifouling Properties. *Langmuir* **2016**, *32*, 10317−10327.

(28) Yu, J.; Jackson, N. E.; Xu, X.; Morgenstern, Y.; Kaufman, Y.; Ruths, M.; de Pablo, J. J.; Tirrell, M. Multivalent Counterions Diminish the Lubricity of Polyelectrolyte Brushes. *Science* **2018**, *360*, 1434−1438.

(29) Zhang, P.; Zhao, C.; Zhao, T.; Liu, M.; Jiang, L. Recent Advances in Bioinspired Gel Surfaces with Superwettability and Special Adhesion. *Adv. Sci.* **2019**, *6*, 1900996.

(30) Wu, J.; Zhang, D.; Zhang, L.; Wu, B.; Xiao, S.; Chen, F.; Fan, P.; Zhong, M.; Tan, J.; Chu, Y.; Yang, J. Long-term Stability and Salt-responsive Behavior of Polyzwitterionic Brushes with Cross-linked Structure. *Prog. Org. Coat.* **2019**, *134*, 153−161.

(31) Dehghani, E. S.; Aghion, S.; Anwand, W.; Consolati, G.; Ferragut, R.; Panzarasa, G. Investigating the Structure of Crosslinked Polymer Brushes (Brush-gels) by Means of Positron Annihilation Spectroscopy. *Eur. Polym. J.* **2018**, *99*, 415−421.

(32) Benetti, E. M.; Sui, X.; Zapotoczny, S.; Vancso, G. J. Surface-Grafted Gel-Brush/Metal Nanoparticle Hybrids. *Adv. Funct. Mater.* **2010**, *20*, 939–944.

(33) Costantini, F.; Benetti, E. M.; Tiggelaar, R. M.; Gardeniers, H. J. G. E.; Reinhoudt, D. N.; Huskens, J.; Vancso, G. J.; Verboom, W. A Brush‐Gel/Metal‐Nanoparticle Hybrid Film as an Efficient Supported Catalyst in Glass Microreactors. *Chem. Eur. J.* **2010**, *16*, 12406–12411.

(34) Li, A.; Ramakrishna, S. N.; Nalam, P. C.; Benetti, E. M.; Spencer, N. D. Stratified Polymer Grafts: Synthesis and Characterization of Layered ‘Brush’ and ‘Gel’ Structures. Adv. Mater. Interfaces **2014**, *1*, 1300007.

(35) Ramakrishna, S. N.; Cirelli, M.; Kooij, E. S.; Gunnewiek, M. K.; Benetti, E. M. Amplified Responsiveness of Multilayered Polymer Grafts: Synergy between Brushes and Hydrogels. *Macromolecules* **2015**, *48*, 7106–7116.

(36) Dehghani, E. S.; Naik, V. V.; Mandal, J.; Spencer, N. D.; Benetti, E. M. Physical Networks of Metal-Ion-Containing Polymer Brushes Show Fully Tunable Swelling, Nanomechanical and Nanotribological Properties. *Macromolecules* **2017**, *50*, 2495–2503.

(37) Dehghani, E. S.; Ramakrishna, S. N.; Spencer, N. D.; Benetti, E. M. Controlled Crosslinking Is a Tool To Precisely Modulate the Nanomechanical and Nanotribological Properties of Polymer Brushes. *Macromolecules* **2017**, *50*, 2932–2941.

(38) Loveless, D. M.; Abu-Lail, N. I.; Kaholek, M.; Zauscher, S.; Craig, S. L. Reversibly Cross-Linked Surface-Grafted Polymer Brushes. *Angew. Chem. Int. Ed.* **2006**, *45*, 7812−7814.

(39) Dehghani, E. S.; Naik, V. V.; Mandal, J.; Spencer, N. D.; Benetti, E. M. Physical Networks of Metal-Ion-Containing Polymer Brushes Show Fully Tunable Swelling, Nanomechanical and Nanotribological Properties. *Macromolecules* **2017**, *50*, 2495−2503.

(40) Mocny, P.; Klok, H.-A. Reversibly Cross-Linking Polymer Brushes Using Interchain Disulfide Bonds. *Macromolecules* **2020**, *53*, 731−740.

(41) Funel, J.-A.; Abele, S. Industrial Applications of the Diels–Alder Reaction. *Angew. Chem. Int. Ed.* **2013**, *52*, 3822−3863.

(42) Gandini, A. The Furan/Maleimide Diels–Alder Reaction: A Versatile Click–Unclick Tool in Macromolecular Synthesis. *Prog. Polym. Sci.* **2013**, *38*, 1−29.

(43) Liu, Y.-L.; Chuo, T.-W. Self-healing Polymers Based on Thermally Reversible Diels–Alder Chemistry. *Polym. Chem.* **2013**, *4*, 2194−2205.

(44) Tasdelen, M. A.; Kiskan, B.; Yagci, Y. Externally Stimulated Click Reactions for Macromolecular Syntheses. *Prog. Polym. Sci.* **2016**, *52*, 19−78.

(45) Vauthier, M.; Jierry, L.; Oliveira, J. C.; Hassouna, L.; Roucoules, V.; Gall, F. B.-L. Interfacial Thermoreversible Chemistry on Functional Coatings: A Focus on the Diels–Alder Reaction. *Adv. Funct. Mater.* **2019**, *29*, 1806765.

(46) Jiang, Y.; Chen, J.; Deng, C.; Suuronen, E. J.; Zhong, Z. Click Hydrogels, Microgels and Nanogels: Emerging Platforms for Drug Delivery and Tissue Engineering. *Biomaterials* **2014**, *35*, 4969−4985.

(47) Arumugam, S.; Orski, S. V.; Locklin, J.; Popik, V. V. Photoreactive Polymer Brushes for High-Density Patterned Surface Derivatization Using a Diels−Alder Photoclick Reaction. *J. Am. Chem. Soc.* **2012**, *134*, 179−182.

(48) Yameen, B.; Rodriguez-Emmenegger, C.; Preuss, C. M.; Pop-Georgievski, O.; Verveniotis, E.; Trouillet, V.; Rezek, B.; Barner-Kowollik, C. A Facile Avenue to Conductive Polymer Brushes *via* Cyclopentadiene–maleimide Diels–Alder Ligation. *Chem. Commun.* **2013**, *49*, 8623−8625.

(49) Gevrek, T. N.; Bilgic, T.; Klok, H.-A.; Sanyal, A. Maleimide-Functionalized Thiol Reactive Copolymer Brushes:Fabrication and Post-Polymerization Modification. *Macromolecules* **2014**, *47*, 7842−7851.

(50) Roling, O.; Mardyukov, A.; Lamping, S.; Vonhören, B.; Rinnen, S.; Arlinghaus, H. F.; Studer, A.; Ravoo, B. J. Surface Patterning with Natural and Synthetic Polymers *via* an Inverse Electron Demand Diels–Alder Reaction Employing Microcontact Chemistry. *Org. Biomol. Chem.* **2014**, *12*, 7828−7835.

(51) Roling, O.; Bruycker, K. D.; Vonhören, B.; Stricker, L.; Körsgen, M.; Arlinghaus, H. F.; Ravoo, B. J.; Du Prez, F. E. Rewritable Polymer Brush Micropatterns Grafted by Triazolinedione Click Chemistry. *Angew. Chem. Int. Ed.* **2015**, *54*, 13126−13129.

(52) Yuksekdag, Y. N.; Gevrek, T. N.; Sanyal, A. Diels-Alder "Clickable" Polymer Brushes: A Versatile Catalyst-Free Conjugation Platform. *ACS Macro Lett.* **2017**, *6*, 415−420.

(53) Ellis, B.; Smith, R. *Polymers: A Property Database*, 2nd ed. Boca Raton: CRC Press, Boca Raton, **2008**, p 690.

(54) Yoshikawa, C.; Goto, A.; Tsujii, Y.; Fukuda, T.; Kimura, T.; Yamamoto, K.; Kishida, A. Protein Repellency of Well-Defined, Concentrated Poly(2-hydroxyethyl methacrylate) Brushes by the Size-Exclusion Effect. *Macromolecules* **2006**, *39*, 2284−2290.

(55) Owens, D. K.; Wendt, R. C. Estimation of the Surface Free Energy of Polymers. *J. Appl. Polym. Sci.* **1969**, *13*, 1741−1747.

(56) Kozbial, A.; Li, Z.; Conaway, C.; McGinley, R.; Dhingra, S.; Vahdat, V.; Zhou, F.; D'Urso, B.; Liu, H.; Li, L. Study on the Surface Energy of Graphene by Contact Angle Measurements. *Langmuir* **2014**, *30*, 8598−8606.

(57) Lange, J.; Rieumont, J.; Davidenko, N.; Sastre, R. Photoinitiated Bulk Polymerization of Furfuryl Methacrylate. Experimental and Kinetic Modelling Results Obtained at Different Temperatures. *Polymer* **1998**, *39*, 2537−2542.

(58) Li, A.; Benetti, E. M.; Tranchida, D.; Clasohm, J. N.; Schönherr, H.; Spencer, N. D. Surface-Grafted, Covalently Cross-Linked Hydrogel Brushes with Tunable Interfacial and Bulk Properties. *Macromolecules* **2011**, *44*, 5344−5351.

(59) Cohen Stuart, M. A.; de Vos, W. M.; Leermakers, F. A. M. Why Surfaces Modified by Flexible Polymers Often Have a Finite Contact Angle for Good Solvents. *Langmuir* **2006**, *22*, 1722−1728.

(60) Parker, A. J.; Kharasch, N. The Scission of The Sulfur-Sulfur Bond. *Chem. Rev.* **1959**, *59*, 583−628.

(61) Chen, T.; Amin, I.; Jordan, R. Patterned Polymer Brushes. *Chem. Soc. Rev.* **2012**, *41*, 3280−3296.

(62) Jung, K.; Corrigan, N.; Ciftci, M.; Xu, J.; Seo, S. E.; Hawker, C. J.; Boyer, C. Designing with Light: Advanced 2D, 3D, and 4D Materials. *Adv. Mater.* **2019**, 1903850.

(63) Wang, S.; Wang, Z.; Li, J.; Li, L.; Hu, W. Surface-grafting Polymers: from Chemistry to Organic Electronics. *Mater. Chem. Front.* **2020**, *4*, 692−714.

(64) Page, Z. A.; Narupai, B.; Pester, C. W.; Zerdan, R. B.; Sokolov, A.; Laitar, D. S.; Mukhopadhyay, S.; Sprague, S.; McGrath, A. J.; Kramer, J. W.; Trefonas, P.; Hawker, C. J. Novel Strategy for Photopatterning Emissive Polymer Brushes for Organic Light Emitting Diode Applications. *ACS Cent. Sci.* **2017**, *3*, 654−661.

(65) Narupai, B.; Page, Z. A.; Treat, N. J.; McGrath, A. J.; Pester, C. W.; Discekici, E. H.; Dolinski, N. D.; Meyers, G. F.; de Alaniz, J. R.; Hawker, C. J. Simultaneous Preparation of Multiple Polymer Brushes under Ambient Conditions using Microliter Volumes. *Angew. Chem. Int. Ed.* **2018**, *57*, 13433−13438.

(66) Chen, C.; Wang, C.-G.; Xiao, L.; Goto, A. Photo-selective Chain End Transformation of Polyacrylate-iodide Using Cysteamine and its Application to Facile Single-step Preparation of Patterned Polymer Brushes. *Chem. Commun.* **2018**, *54*, 13738−13741.

(67) Chen, C.; Wang, C.-G.; Guan, W.; Goto, A. A Photo-selective Chain-end Modification of Polyacrylate-iodide and its Application in Patterned Polymer Brush Synthesis. *Polym. Chem.* **2019**, *10*, 5913−5919.

for Table of Contents use only